ASSESSING THE ACCURACY AND VARIABILITY OF ESTIMATING SNOW WATER EQUIVALENT FROM LAKE WATER PRESSURE

by

Erich Stefan Schreier

A thesis submitted in partial fulfillment
of the requirements for the degree

of

Master of Science

in

Earth Science

MONTANA STATE UNIVERSITY
Bozeman, Montana

May 2025

©COPYRIGHT

by

Erich Stefan Schreier

2025

All Rights Reserve

ACKNOWLEDGEMENTS

This thesis is the culmination of two years of support from colleagues, friends, and family. Dr. Eric Sproles saw the potential in this research and graciously took me on as a member of the GeoSWIRL team and the Geospatial Core Facility. Dr. Annie Burgess provided valuable insights into operational water forecasting, which helped to focus the goals of this research. Dr. Kelsey Jensco contributed his extensive experience in hydrologic monitoring and climatic controls on the snowpack, helping build a solid understanding of the limitations and advantages of the novel method we tested. I am incredibly thankful for the guidance and support from my committee.

I would like to thank Niko Hinz for his hard work and expertise in the field, and for assisting in the processing of the LiDAR data. Bryce Gordon also provided invaluable assistance in the field.

I would like to thank the entire Geospatial Core Facility and GeoSWIRL team for their support and assistance throughout this project, and to the Geospatial Core Facility for funding this research.

Finally, to my partner Erin, whose encouragement, patience, and zest for life made every moment of this research journey worth it.

TABLE OF CONTENTS

1. INTRODUCTION 1

2. ASSESSING THE ACCURACY AND VARIABILITY OF ESTIMATING SNOW WATER EQUIVALENT FROM LAKE WATER PRESSURE 5

Contribution of Authors and Co-Authors 5
Manuscript Information 6
1 Introduction 7
2 Materials and Methods 10
2.1 Field site and data collection 10
3 Results 15
3.1 Pressure trends and data smoothing 15
3.1 Lake pressure SWE estimates 18
3.3 Manual observations 24
3.4 LiDAR snow depth 29
3.5 Loss of lake ice snowpack 33
4 Discussion 34
4.1 Future considerations 34
4.1 Limitations 36
5 Conclusion 37

3. CONCLUSION 39

CUMULATIVE REFERENCES CITED 40

LIST OF TABLES

Table Page

1. Table 1. Median event values and error, and the cumulative season SWE, from the raw pressure data, moving median filter, and STL filter. The raw pressure results show a much higher dP_D uncertainty than both moving median and STL results. Poor $\dot{D}_1$ and $\dot{D}_2$ R^2 values for the raw pressure data reflect the challenge of estimating linear drainage fits with noisy pressure data, and the median moving and STL filters show a marked improvement in drainage rate estimation. 22

2. Table 2. Count of manual SWE and depth observations collected during each sampling date. Sample size varies based on team capacity for each day, and no samples were collected on March 20 over the lake surface due to standing water and hazardous ice conditions. 25

LIST OF FIGURES

Figure Page

1. Figure 1. Location of Mystic Lake in Gallatin County, Montana (red dot) (a). Aerial imagery of Mystic Lake displaying locations of the pressure transducers and AWS (b). Photo of Mystic Lake, looking south, taken on March 20, 2024 (c). The transducers were placed in stilling wells and inserted into the lakebed (d). 11

2. Figure 2. Conceptual plot displaying the components of a hypothetical water pressure signal (black line) used to estimate SWE corresponding to observed snow accumulation (blue bars). It is important to note that drainage rate increases in the transition from Ḋ1to Ḋ2 as a function of extra pressure from snow loading. 14

3. Figure 3. Time series of water pressure collected at all locations (top plot is the pond location), the average of the two sensors in Mystic Lake (lines), and snow depth recorded at the AWS as blue bars. 16

4. Figure 4. Mystic Average pressure time series highlighting the observed diurnal pressure cycle prior to a snow event on February 26-27. The time series is colored red when air temperature is greater than 0°C, and blue when it is equal to or less than 0°C. Observed snow accumulation from the AWS is displayed as blue bars. Note that the daily cycle contains a rapid rise and fall of the pressure signal of several centimeters. 17

5. Figure 5. Correlation between the rate of change of air temperature, when air temperature is equal to or greater than 0°C, and the rate of change of water pressure. Using the rate of change shows that increases in temperature are correlated to increases in pressure. 18

6. Figure 6. STL decomposes the raw Mystic Average pressure signal (top) into trend (middle) and seasonal (bottom) components. The trend component is used for estimating SWE, and the seasonal component is used to further investigate the diurnal cycle. 20

7. Figure 7. Correlation between air temperature and the STL seasonal component. Above 0°C, air temperature correlates more significantly (R^2 = 0.30, p-value = 0.000) with the diurnal cycle captured by STL than air temperature ≥ 0°C (R^2 = 0.05, p-value = 0.000). 21

LIST OF FIGURES CONTINUED

Figure Page

8. Figure 8. Estimation of pre-snow drainage (pink), post-snow drainage (green), and the total drainage component *(dP_D,* dotted pink line) for Mystic Lake Average pressure shown for the February 26 snow event for raw pressure (a), moving median (b), and STL (c). Linear fit estimates for drainage rates are significantly improved by filtering the data..... 23

9. Figure 9. Raw pressure (black), moving median (green), and STL (blue) time series displaying a continued decreasing trend during snow events on March 24 and March 26-27. The pressure response to snow loading was likely muted due to a partially unfrozen lake surface. 24

10. Figure 10. Box plots of SWE (a), density (b), and depth (c) recorded by sampling date and surface. Density was back calculated from SWE and depth. Ground surfaces steadily accumulated snow throughout the study, while the lake surface reaches a maximum SWE and depth on February 17. 26

11. Figure 11. Change in SWE (ΔSWE) observed in between field sampling dates. The negative changes observed on the lake surface from Feb. 28 and Mar. 20 are the result of the complete loss of the lake surface snowpack. The height of each bar represents the total observed SWE on Mar. 27. All three water pressure series overestimate manual SWE observed on the lake surface, but STL pressure estimates most closely represent what was observed over the ground at the study site and at the Lick Creek SNOTEL site. 29

12. Figure 12. LiDAR snow depth, and snow depth recorded at the AWS, by sampling date. The location of the AWS in a forest clearing likely contributed to the deeper snowpack observed there relative to the rest of the study site. Snow depth over the lake surface was comparable to the study site on February 01 and experienced a similar increase in depth from March 20 to 27 of 8cm, compared to 9cm across the study site, but the loss of the snowpack over the lake surface on March 20 reveals an enhanced rate of snow loss not observed at any other area of the study site. 31

13. Figure 13. Snow depth retrieved from LiDAR on March 27. Vegetation and negative values are masked to highlight where snow is and is not present at the study site. The lake surface displays more homogenous snow depth compared to its surroundings. Forest clearings show the deepest snowpack in dark purple. 32

ABSTRACT

Seasonal snowpack is a crucial global water resource, but measuring it accurately poses challenges. Measurements of snow water equivalent (SWE) from existing instruments are susceptible to significant bias and often provide data only at the point scale. The global network of SWE sensors is sparse and bias towards lower elevations in the mountains, limiting their effectiveness in informing hydrologic models and forecasts. A promising new method has been proposed to estimate SWE from lake pressure in frozen alpine lakes. To gain a more complete understanding of the capabilities of this method, we conducted an alpine study site at Mystic Lake (45.54, -110.93) in Southwest Montana, USA. We present how noise in the water pressure signal can add significant uncertainty to SWE methods, and we present methods for smoothing the data to achieve more reliable estimates in employing this method to measure SWE. We find that there is substantial variability between SWE observed over the ice surface and adjacent ground surfaces during the study period, underscoring the challenges of measuring snow in the mountains. The results of this study demonstrate that estimating SWE from lake water pressure can provide valuable insights into basin hydrology and easy-to-implement observations of SWE. However, careful consideration and site-specific planning are requisite for accurate and representative SWE estimates.

INTRODUCTION

Seasonal snowfall supports the water supply for 20% of the human population around the world (Barnett et al. 2005). In the western United States, up to 70% of streamflow is supplied by melting snow (Li et al. 2017), supporting 60 million people (Bales et al. 2006) and valued at over a trillion dollars (Sturm et al. 2017). Mountain snowpack is declining (Notarnicola, 2022), and an estimated loss of 25% of snow water equivalent (SWE) is expected by 2050 in the Western United States (Siirila-Woodburn et al., 2021). SWE, a measure of how much water is stored in the snowpack, is an important indicator for water resource forecasting and modelling (Yao et al. 2018). However, measuring the spatiotemporal distribution of SWE in mountainous regions is a significant challenge in snow hydrology (Dozier et al., 2016; Cho et al., 2021). Current measurements remain too sparse, spatially and temporarily, to be sufficiently representative of the mountain snowpack (Sturm et al., 2010; Herbert et al., 2024). There are currently over 1,100 manual snow course survey sites and over 850 automated SNOTEL sites in operation in the United States (NRCS, 2024). Snow course observations, which are manually collected, are temporally restricted to the few times a year each site is sampled. Automated SNOTEL sites do collect continuous measurements throughout the winter, primarily using snow pillows. These devices are a sealed bladder filled with an anti-freeze fluid, and the fluid pressure fluctuates in response to the mass of snow atop the snow pillow. While informative, the spatial resolution of individual sites, and the spatial distribution of the SNOTEL network, present limitations. The point observations returned from SNOTEL sites were found to inadequately represent 1 km2 grid cells surrounding a site with a bias of up to 200% (Molotch and Bales, 2005). The distribution of SNOTEL sites does not cover the higher mountain elevations despite these areas harboring the

most SWE and surface water input volume per square meter (Hammond et al., 2023). Furthermore, even basins that are well monitored are subject to significant forecast errors. For example, one watershed in the Sierra Nevada mountains of California was found to have a median error in predicted runoff of 18%, with a maximum error of 129% (Dozier, 2011).

To produce more reliable runoff forecasts and improve management of vital snow water resources, a more extensive network of in-situ SWE measurements is needed (Li et al., 2019). Existing methods and instruments, however, have significant limitations for operation in mountain areas. Snow pillows and scales, known as the most common fixed instrument for monitoring SWE (Taheri and Abdolmajid, 2022), require significant ground disturbance and can be cost-prohibitive (Stranden et al. 2015). Above ground neutron and gamma ray sensors provide other approaches to measure SWE but can be similarly cost prohibitive and are limited to snowpacks with a SWE of ~15cm and ~60cm respectively (Pritchard et al. 2021). This measurement limitation for both neutron and gamma ray sensors may restrict their use in deeper, mountain snowpacks.

Building on an observation made by van der Kamp et al. (2008), Pritchard et al. (2021) proposed a new method of measuring SWE that could help reduce the data limitations in mountainous areas. The method utilizes natural lakes to observe changes in the snowpack SWE by continuously measuring lake water pressure with autonomous pressure sensors. Pritchard et al. (2021) hypothesized that, under freezing conditions, lake pressure would respond to the increased mass of accumulated snow on its ice surface, similar to the function of a snow pillow. Using pressure transducers in natural lakes offers multiple advantages over previously established methods. Pressure transducers are commercially available and inexpensive compared

to other SWE monitoring instruments. They are simple to install with minimum disruption to the surrounding environment. There is an abundance of high-elevation lakes where measurements could be continuously collected in locations that are not feasible to install and maintain other instruments. Furthermore, the measurement footprint of this method is the entire lake surface. Pritchard et al. (2021) found in their study that snow-induced changes in lake water pressure yielded SWE measurements similar to that recorded at nearby weather stations, with uncertainty comparable to or better than other SWE monitoring instruments. Pritchard et al. (2021) demonstrate that this affordable and easy-to-implement method shows great promise in expanding the spatial coverage of SWE monitoring networks in mountain snowpacks. Before this method can be implemented in monitoring networks and used for water resource forecasting, it is crucial to understand the accuracy and spatial representativeness of SWE estimates from lake water pressure. Additionally, further investigation is required into whether the ice surface introduces bias into SWE estimates.

Here, we apply the lake pressure method to evaluate its accuracy and representativeness at a field site in southwestern Montana. We find that noise from non-snow-induced pressure changes can introduce considerable error in calculating SWE from lake pressure, and we test two common data filtering techniques for their effectiveness in reducing estimate uncertainty. We collected in-situ SWE and snow depth measurements over the lake ice surface and the surrounding ground surfaces to assess the accuracy and spatial representation of lake pressure SWE estimates. Snow depth from LiDAR was acquired to reveal the spatiotemporal pattern of snow accumulation at a finer scale than manual observation can achieve. The goal of this study is to investigate the constraints on the physical setting in which this method can be applied,

further define method limitations, and gain a better understanding of the applicability of the lake pressure method for use in SWE monitoring networks.

ASSESSING THE ACCURACY AND VARIABILITY OF ESTIMATING SNOW WATER EQUIVALENT FROM LAKE WATER PRESSURE

Contribution of Authors and Co-Authors

Manuscript in Chapter 2

Author: Erich Stefan Schreier

Contributions: Conceptualization, field investigation, analyses, methodology, writing

Co-Author: Eric Sproles

Contributions: Conceptualization, methodology development, data analysis support, writing review and editing

Co-Author: Nioclas Hinz

Contributions: Field investigation, data analysis support

Manuscript Information

Erich Schreier, Eric Sproles, Nioclas Hinz

Status of Manuscript:
☒ Prepared for submission to a peer-reviewed journal
☐ Officially submitted to a peer-reviewed journal
☐ Accepted by a peer-reviewed journal
☐ Published in a peer-reviewed journal

1 Introduction

Seasonal snowfall supports the water supply for 20% of the human population around the world (Barnett et al. 2005). In the western United States, up to 70% of streamflow is supplied by melting snow (Li et al. 2017), supporting 60 million people (Bales et al. 2006) and valued at over a trillion dollars (Sturm et al. 2017). Mountain snowpack is declining (Notarnicola, 2022), and an estimated loss of 25% of snow water equivalent (SWE) is expected by 2050 in the Western United States (Siirila-Woodburn et al., 2021). SWE, a measure of how much water is stored in the snowpack, is an important indicator for water resource forecasting and modelling (Yao et al. 2018). However, measuring the spatiotemporal distribution of SWE in mountainous regions is a significant challenge in snow hydrology (Dozier et al., 2016; Cho et al., 2021). Current measurements remain too sparse, spatially and temporarily, to be sufficiently representative of the mountain snowpack (Sturm et al., 2010; Herbert et al., 2024). There are currently over 1,100 manual snow course survey sites and over 850 automated SNOTEL sites in operation in the United States (NRCS, 2024). Snow course observations, which are manually collected, are temporally restricted to the few times a year each site is sampled. Automated SNOTEL sites do collect continuous measurements throughout the winter, primarily using snow pillows. These devices are a sealed bladder filled with an anti-freeze fluid, and the fluid pressure fluctuates in response to the mass of snow atop the snow pillow. While informative, the spatial resolution of individual sites, and the spatial distribution of the SNOTEL network, present limitations. The point observations returned from SNOTEL sites were found to inadequately represent 1 km^2 grid cells surrounding a site with a bias of up to 200% (Molotch and Bales, 2005). The distribution of SNOTEL sites does not cover the higher mountain elevations despite these areas harboring the

most SWE and surface water input volume per square meter (Hammond et al., 2023). Furthermore, even basins that are well monitored are subject to significant forecast errors. For example, one watershed in the Sierra Nevada mountains of California was found to have a median error in predicted runoff of 18%, with a maximum error of 129% (Dozier, 2011).

To produce more reliable runoff forecasts and improve management of vital snow water resources, a more extensive network of in-situ SWE measurements is needed (Li et al., 2019). Existing methods and instruments, however, have significant limitations for operation in mountain areas. Snow pillows and scales, known as the most common fixed instrument for monitoring SWE (Taheri and Abdolmajid, 2022), require significant ground disturbance and can be cost-prohibitive (Stranden et al. 2015). Above ground neutron and gamma ray sensors provide other approaches to measure SWE but can be similarly cost prohibitive and are limited to snowpacks with a SWE of ~15cm and ~60cm respectively (Pritchard et al. 2021). This measurement limitation for both neutron and gamma ray sensors may restrict their use in deeper, mountain snowpacks.

Building on an observation made by van der Kamp et al. (2008), Pritchard et al. (2021) proposed a new method of measuring SWE that could help reduce the data limitations in mountainous areas. The method utilizes natural lakes to observe changes in the snowpack SWE by continuously measuring lake water pressure with autonomous pressure sensors. Pritchard et al. (2021) hypothesized that, under freezing conditions, lake pressure would respond to the increased mass of accumulated snow on its ice surface, similar to the function of a snow pillow. Using pressure transducers in natural lakes offers multiple advantages over previously established methods. Pressure transducers are commercially available and inexpensive compared

to other SWE monitoring instruments. They are simple to install with minimum disruption to the surrounding environment. There is an abundance of high-elevation lakes where measurements could be continuously collected in locations that are not feasible to install and maintain other instruments. Furthermore, the measurement footprint of this method is the entire lake surface. Pritchard et al. (2021) found in their study that snow-induced changes in lake water pressure yielded SWE measurements similar to that recorded at nearby weather stations, with uncertainty comparable to or better than other SWE monitoring instruments. Pritchard et al. (2021) demonstrate that this affordable and easy-to-implement method shows great promise in expanding the spatial coverage of SWE monitoring networks in mountain snowpacks. Before this method can be implemented in monitoring networks and used for water resource forecasting, it is crucial to understand the accuracy and spatial representativeness of SWE estimates from lake water pressure. Additionally, further investigation is required into whether the ice surface introduces bias into SWE estimates.

Here, we apply the lake pressure method to evaluate its accuracy and representativeness at a field site in southwestern Montana. We find that noise from non-snow-induced pressure changes can introduce considerable error in calculating SWE from lake pressure, and we test two common data filtering techniques for their effectiveness in reducing estimate uncertainty. We collected in-situ SWE and snow depth measurements over the lake ice surface and the surrounding ground surfaces to assess the accuracy and spatial representation of lake pressure SWE estimates. Snow depth from LiDAR was acquired to reveal the spatiotemporal pattern of snow accumulation at a finer scale than manual observation can achieve. The goal of this study is to investigate the constraints on the physical setting in which this method can be applied, further define method

limitations, and gain a better understanding of the applicability of the lake pressure method for use in SWE monitoring networks.

2 Materials and Methods

2.1 Field site and data collection

This study was conducted at Mystic Lake in Southwest Montana, USA (45.5491, -110.9359, 1950 m.a.s.l; Figure 1). Bozeman Creek, which originates from Mystic Lake, provides the nearby city of Bozeman with ~40% of its water supply, yet the entire watershed contains no snow monitoring instruments. Mystic Lake serves as an ideal location to fill a significant data gap for local water managers in an unmonitored watershed. The site was also selected for its safe and reliable winter access. A vehicle-restricted, 16km gravel road leads to the lake and is maintained for cross-country skiing, which allows access to the site even in difficult travel conditions. In snow-free conditions, the site was accessed via bicycle. Directly to the west of the Bozeman Creek watershed is Hyalite Creek. In Hyalite Creek watershed, the Lick Creek SNOTEL site sits at an elevation of 2090 m.a.s.l, ~5.5km to the southwest of Mystic Lake, and provides the most geographically representative comparison of SWE measurements at Mystic Lake.

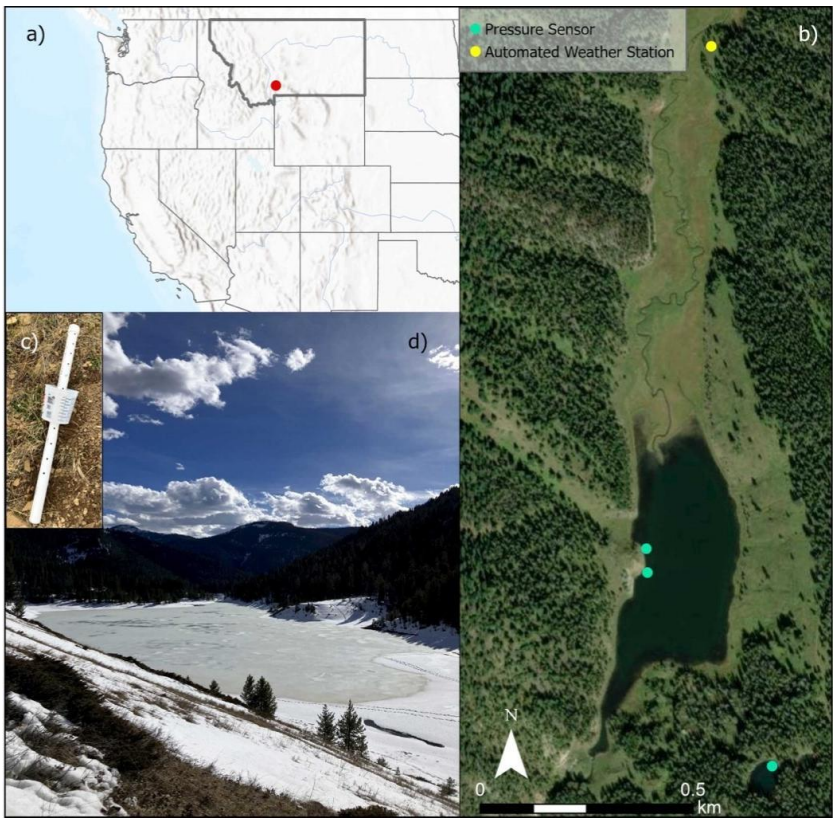


Figure 1. Location of Mystic Lake in Gallatin County, Montana (red dot) (a). Aerial imagery of Mystic Lake displaying locations of the pressure transducers and AWS (b). Photo of Mystic Lake, looking south, taken on March 20, 2024 (c). The transducers were placed in stilling wells and inserted into the lakebed (d).

We deployed four commercially available HOBO U20L water level loggers (Onset, 2025) at the study site to collect data hourly. Two sensors were placed in Mystic Lake which allowed for averaging of the time series to reduce transient noise (Pritchard et al. 2021). Due to the time constraints of gaining proper permits for our research, the lake was already partially frozen over when the sensors were placed in mid-November 2023. This limited the placement of the sensors in Mystic Lake, which were installed close together. One pressure sensor was placed in a small pond near the lake to test the applicability of this method in a very small body of water. The sensors were installed by situating them in a stilling well ~1m in height, which was inserted into

the lake and pond bed surface to help reduce the potential for the sensors to settle into the lakebed or drift in location (Figure 1d). A fourth pressure transducer was installed at the site adjacent to the lake to measure ambient barometric pressure to correct lake pressure. An automated weather station (AWS) was installed at the study site, which recorded hourly snow depth, wind speed and direction, air temperature, relative humidity, and net radiation. The AWS was established in a clearing in the large meadow at the study site to closely represent conditions at the lake.

This project's scope spanned the 2023-2024 winter season, in which five field sampling days were conducted. Field sampling occurred on February 1, 17, and 27, and March 20, and 27. The field sampling schedule was flexible so that visits could be conducted shortly following a snow event to closely compare field observations with snow events detected in the water pressure signal. During all site visits, a federal snow sampler was used to observe SWE and snow depth along a randomized sampling grid over both the lake ice and surrounding ground surfaces. LiDAR data was obtained on February 1, March 20, and 27 via a GreenValley International LiAir V70 sensor (vertical accuracy = ±5cm) mounted to a DJI Matrice UAV, and snow depth was calculated by subtracting the elevation from a bare ground dataset collected in June, from the snow-covered datasets. The LiDAR datasets were processed to a resolution of 50cm, which has been shown to be of sufficient size to capture snow depth variability in complex terrain (Miller et al., 2022). Because the ice surface elevation can fluctuate, we needed to estimate the ice surface elevation in order to derive snow depth from the LiDAR data. This was done by estimating the bare ground lake elevation from 5cm contour lines and subtracting both the median LiDAR depth change and the median manually observed snow depth from this value.

The LiDAR depth change was subtracted because the bare ground water level, collected in the spring, was found to be at a higher elevation than the ice surfaces due to the increase in lake volume from melt runoff.

2.2 Calculating SWE estimates and uncertainty

To estimate SWE, we parallel the methodology of Pritchard et al. (2021), which accounts for the dynamic nature of a water body's drainage during a snow event and measurement uncertainty. Unlike the closed system of a snow pillow, a lake is a natural system in which water is constantly flowing in and out of the system. In the winter, under sustained freezing conditions, a net loss of water from the lake is expected, which translates to a continuous and steady drop in water pressure. Snow loading on the lake temporarily increases water pressure, ΔP, but the drainage component of the pressure signal, $d\dot{D}$, must be accounted for more accurate estimates of SWE. Since drainage is not constant and evolves with snow loading, it must be calculated separately for each event. This is done by fitting a linear trend to dry periods immediately before, $\dot{D}_1$, and after, $\dot{D}_2$, after a snow event.

$$\frac{dD}{dP} = \frac{\dot{D_2} - \dot{D_1}}{\Delta P}$$

These rates allow us to estimate drainage at all time steps during the event, $\dot{D}(t,P)$, and after a snow event, $\dot{D}dt$, as

$$\dot{D}(t,P) = \dot{D}_1 + (d\dot{D}/dP)\,[P(t) - P_{t0}].$$

By integrating the drainage component, dP_D, over the event duration and subtracting it from the total pressure change, we isolate the pressure change due to SWE, dP_{SWE}, as

$$dP_D(t) = \int_{t0}^{t} \dot{D}\,dt,$$

$$dP_{SWE} = dP - dP_D.$$

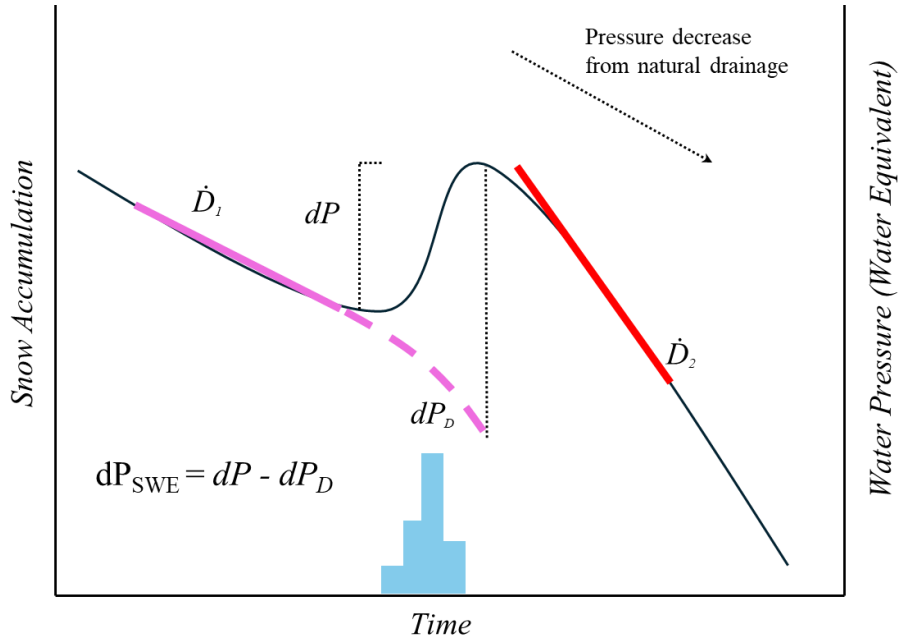


Figure 2. Conceptual plot displaying the components of a hypothetical water pressure signal (black line) used to estimate SWE corresponding to observed snow accumulation (blue bars). It is important to note that drainage rate increases in the transition from Ḋ1to Ḋ2 as a function of extra pressure from snow loading.

Uncertainty in dP_D comes from the combined uncertainty of the $\dot{D}_1$ and $\dot{D}_2$ linear fits and instrumental uncertainty. We calculate drainage uncertainty, ε_d, to two using standard error prorogation as

$$\varepsilon_d = 2\left(\varepsilon_{\dot{D}_1}{}^2 + \varepsilon_{\dot{D}_2}{}^2 + \varepsilon_i{}^2 + \varepsilon_y{}^2\right)^{1/2}$$

where $\varepsilon_{\dot{D}_1}$ and $\varepsilon_{\dot{D}_2}$ are the standard errors in the linear fits for the pre-snow and post-snow drainage rates, ε_y is the standard error of the y estimates for each linear fit and ε_i is the

instrumental error which was calculated from a laboratory test to be 0.01cm. The uncertainty in event SWE, ε_{SWE}, is calculated as,

$$\varepsilon_{SWE} = 2\left(\varepsilon_d{}^2 + \varepsilon_i{}^2 + \varepsilon_y{}^2\right)^{1/2}$$

It is noteworthy that this study took place during one of the lowest snow years on record (1965). In January and February, the Lick Creek SNOTEL recorded a record-low SWE for 55 days, almost the entire two months, except for five days. Peak SWE in 2024 was bolstered by significant snow in late April and May, which we were not able to detect in the pressure signal, most likely due to elevated inflows into a partially thawed Mystic Lake, the combination of which likely muted the snow signal. Because of this record-low winter during sampling, we faced the challenges associated with sampling a shallow snowpack. Measuring snow in the field is challenging, and it has been found that the accuracy of the Federal sampler, which we used to manually collect SWE observations, is significantly limited in shallow snowpacks (Dixon and Boon, 2012; López-Moreno et al., 2020). This introduces an unknown source of error in the manual samples.

3 Results

3.1 Pressure trends and data smoothing

Both sensors in Mystic Lake and the sensor in the pond recorded a gradual decrease in pressure from mid-March, which was similarly observed by Pritchard et al. (2021), and represents the natural drainage from the lake (Figures 2 and 3). During this period, snow events are discernable by short-term increases in pressure that coincide with snow events detected by the AWS. Water

pressure then begins to increase in late March, marked by five discernable snow events that coincide with a sharp decrease in water pressure. We believe that the lake surface was not frozen during these snow events. Therefore, the colder temperatures during the snow events reduced the rate of melt runoff which corresponds to a decrease in water pressure. The water pressure then spikes in the days following these late spring snow events, which we believe is caused by rapid inflow from melt runoff.

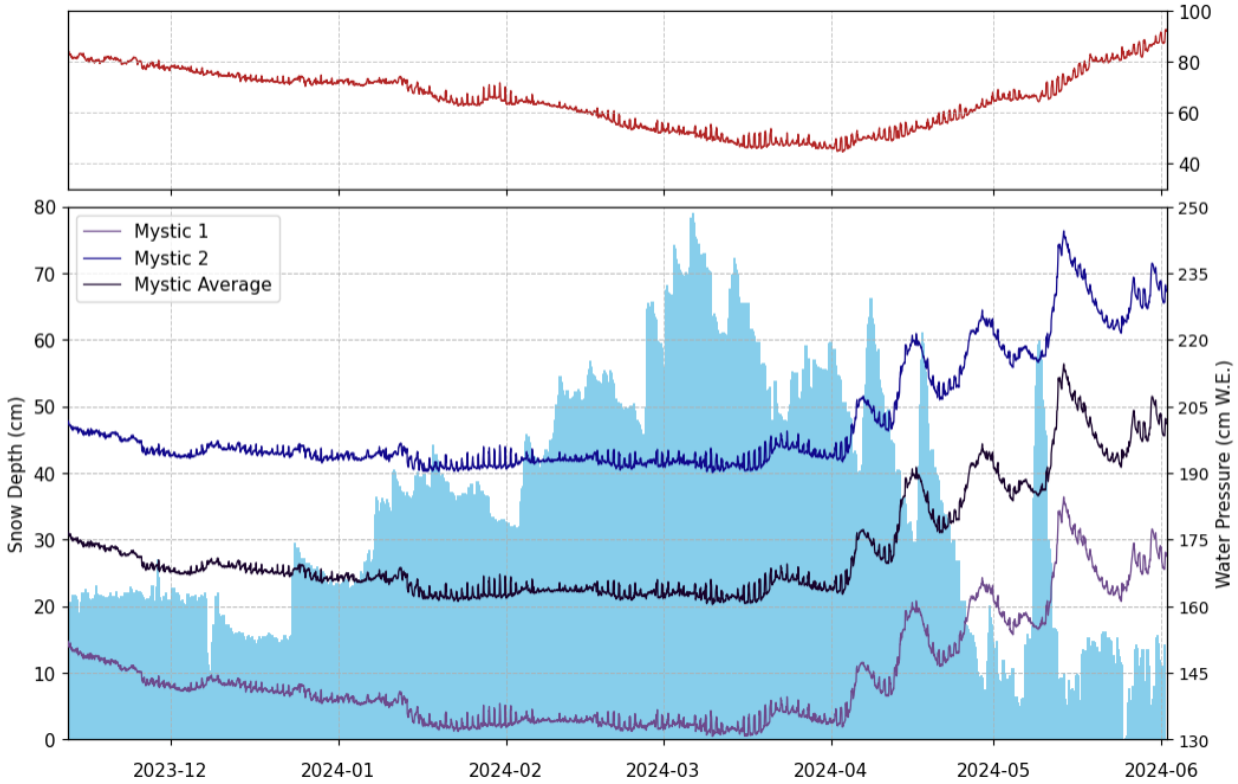


Figure 3. Time series of water pressure collected at all locations (top plot is the pond location), the average of the two sensors in Mystic Lake (lines), and snow depth recorded at the AWS as blue bars.

All three pressure transducers recorded a diurnal cycle of a rapid increase and decrease in water pressure (Figure 4). We found that changes in air temperature were highly correlated with

changes in water pressure with a Pearson correlation coefficient of 0.62, which was strengthened to 0.81 when air temperature was greater than or equal to 0°C (Figure 5). This points to a strong relationship between temperature and the diurnal pressure cycle. Pritchard et al. (2021) found that transient pressure spikes may result from high winds during snow events. Although wind may have played a role during individual snow events, no significant correlation was found between wind speeds and water pressure in our study.

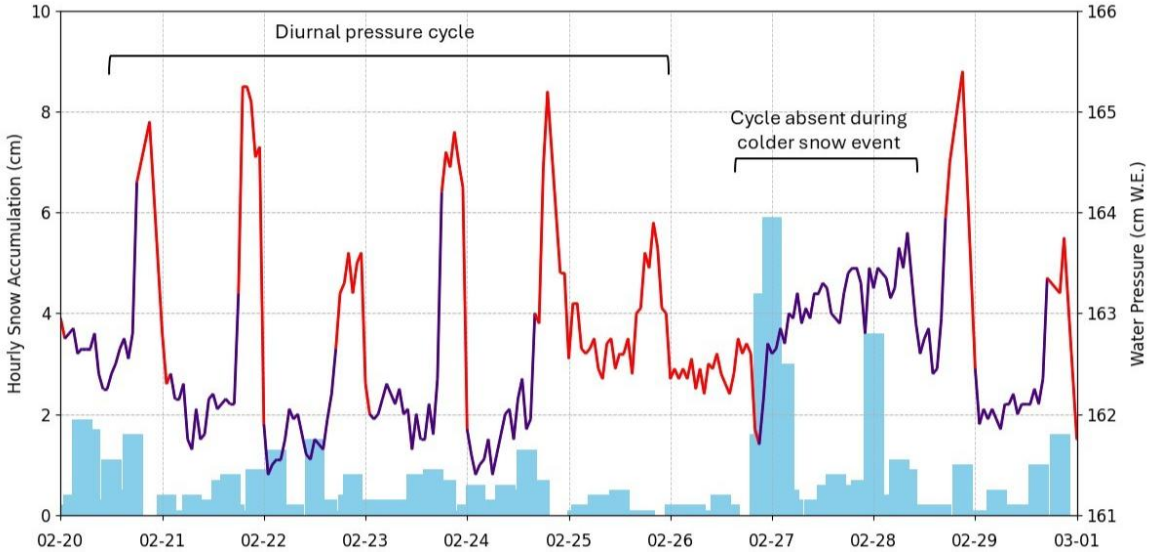


Figure 4. Mystic Average pressure time series highlighting the observed diurnal pressure cycle prior to a snow event on February 26-27. The time series is colored red when air temperature is greater than 0°C, and blue when it is equal to or less than 0°C. Observed snow accumulation from the AWS is displayed as blue bars. Note that the daily cycle contains a rapid rise and fall of the pressure signal of several centimeters.

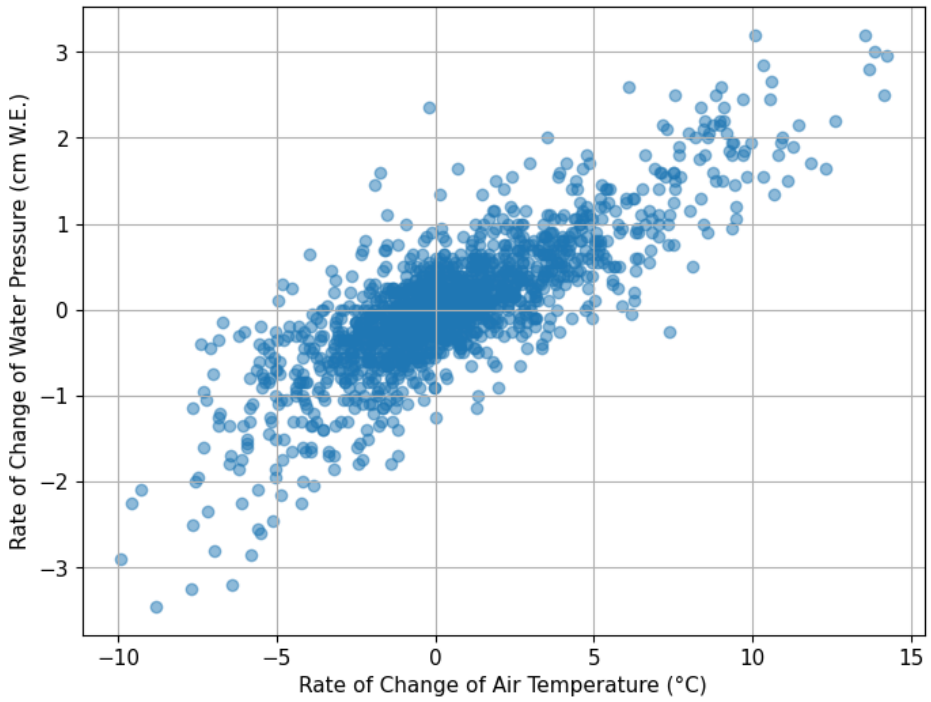


Figure 5. Correlation between the rate of change of air temperature, when air temperature is equal to or greater than 0°C, and the rate of change of water pressure. Using the rate of change shows that increases in temperature are correlated to increases in pressure.

3.1 Lake pressure SWE estimates

We present only the average of the two sensors in Mystic Lake, as we found that the sensor in the pond only recorded a single discernable snow event, so it is not considered in the analysis. It was observed that a large portion of the pond remained unfrozen near an inlet throughout the study, preventing snow from accumulating on its surface. We identified 15 snow events in the Mystic Lake pressure time series.

In calculating SWE from the average of the two Mystic Lake sensors, we found considerable uncertainty in the SWE estimates. Average snow event SWE uncertainty was calculated as ± 4.027cm, which is 168% of the average snow event SWE estimate of 2.396cm (Table 1). The

maximum event uncertainty was over 380%. The low drainage rate R^2 values, with an average $\dot{D}_1$ R^2 value of 0.18 and an average $\dot{D}_2$ R^2 value of 0.24, indicate that the noisy data presents challenges in estimating pre-snow and post-snow drainage rates with linear fits. This is further supported by the substantial error in the drainage component with an average dP_D error of ±1.89cm (Table 1). Such large uncertainties complicate the assessment of the accuracy of SWE estimates from the lake pressure method.

To reduce this uncertainty, we employed a moving median filter and seasonal-trend decomposition (STL) to reduce noise in the pressure signal. Moving average filtering is a common technique in hydrologic time series analysis to smooth short-term fluctuations (Almazroui and Sen, 2020). In this study, we use a moving median instead of a moving average to make the filtered data more robust to large pressure spikes. A moving window length of 24 hours, corresponding to one day for our hourly pressure time series, was used to isolate the effects of the daily spikes without over-smoothing the data. STL decomposes the time series into trend, seasonal, and residual components using LOESS (Locally Estimated Scatterplot Smoothing), a non-parametric regression method that fits locally weighted polynomials to a designated seasonal period, which in our study is 24 hours (Figure 6). The resulting trend component from STL captures changes in the time series that are not influenced by the observed diurnal cycle. We selected this approach over other filters due to its simplicity in application, parameter selection, and robustness to outliers (Cleveland et al., 1990). Furthermore, the seasonal component derived from STL allows for further investigation into the diurnal pattern. Air temperature exhibited a moderate correlation with the seasonal component of pressure data

(R^2 = 0.18), which increased modestly when air temperature was ³ 0°C (R^2 = 0.3). A greater significance for above-freezing temperatures indicates that warmer temperatures are more correlated with the observed diurnal cycle (Figure 7).

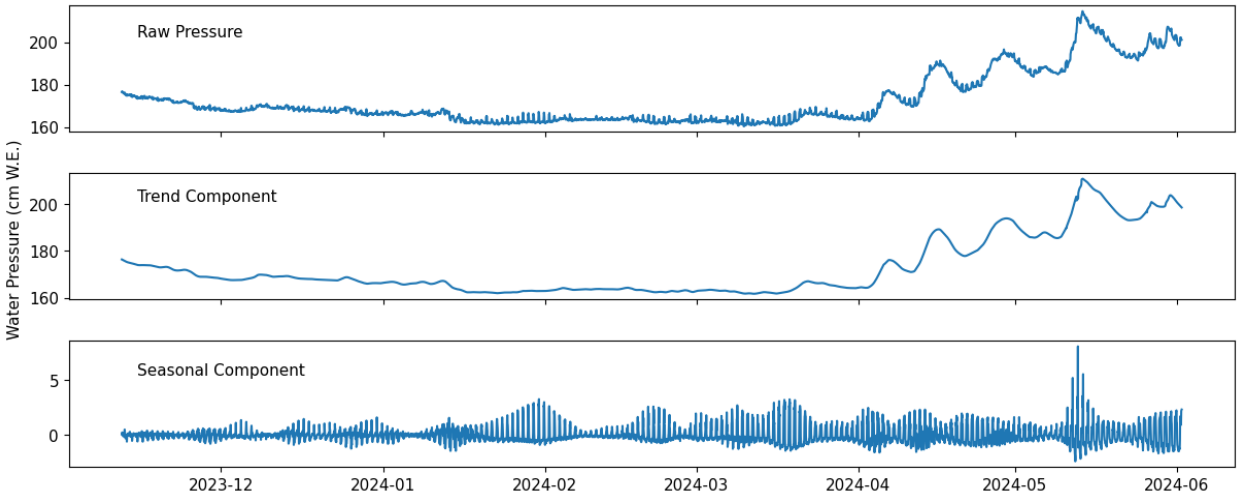


Figure 6. STL decomposes the raw Mystic Average pressure signal (top) into trend (middle) and seasonal (bottom) components. The trend component is used for estimating SWE, and the seasonal component is used to further investigate the diurnal cycle.

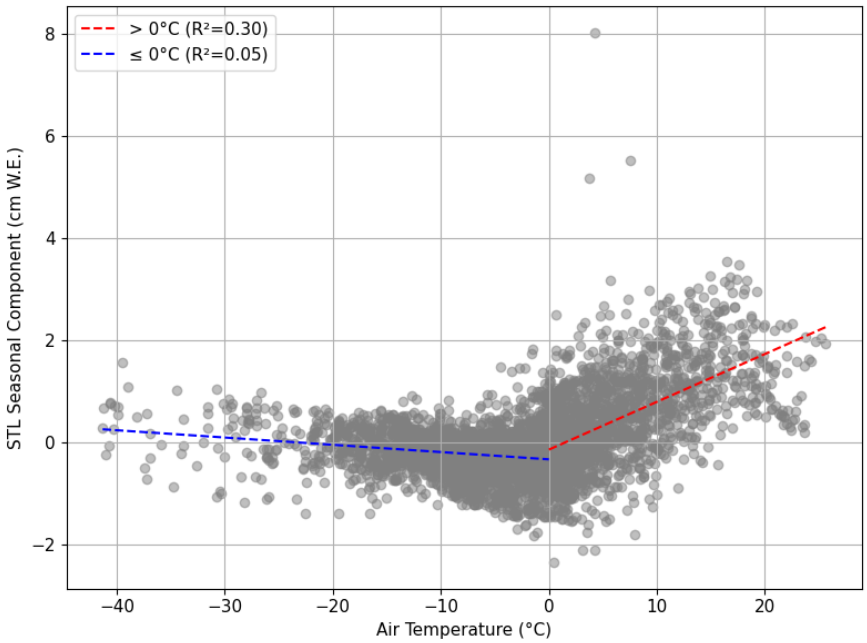


Figure 7. Correlation between air temperature and the STL seasonal component. Above 0°C, air temperature correlates more significantly (R2 = 0.30, p-value = 0.000) with the diurnal cycle captured by STL than air temperature ≥ 0°C (R2 = 0.05, p-value = 0.000).

Event Estimates	Raw Pressure	Moving Median	STL
$\dot{D}_1$ (cm W.E./ hour)	-0.017 ± 0.012	-0.012 ± 0.002	-0.009 ± 0.001
$\dot{D}_1$ R^2	0.18	0.78	0.95
$\dot{D}_2$ (cm W.E./ hour)	-0.040 ± 0.019	-0.030 ± 0.004	-0.022 ± 0.001
$\dot{D}_2$ R^2	0.24	0.62	0.94
dP_D (cm W.E.)	-1.460 ± 1.885	-1.032 ± 0.024	-0.839 ± 0.022
dP (cm W.E.)	0.936	0.775	0.611
dP_{SWE} (cm W.E.)	2.396 ± 4.027	1.807 ± 1.139	1.45 ± 1.19
Smoothing error (cm W.E.)	-	± 0.569	± 0.594
Cumulative Season SWE (cm W.E.)	33.539	25.291	20.297

Table 1. Median event values and error, and the cumulative season SWE, from the raw pressure data, moving median filter, and STL filter. The raw pressure results show a much higher dP_D uncertainty than both moving median and STL results. Poor $\dot{D}_1$ and $\dot{D}_2$ R^2 values for the raw pressure data reflect the challenge of estimating linear drainage fits with noisy pressure data, and the median moving and STL filters show a marked improvement in drainage rate estimation.

To account for uncertainty introduced by filtering the data, we calculated the root mean square error (RMSE) for each filter over the duration of individual snow events and incorporated it into the overall SWE uncertainty. The average smoothing errors were ±0.57 cm for the rolling median and ±0.59 cm for STL. Despite the additional filtering error, we saw a substantial reduction in SWE estimate uncertainty by applying the filters. The moving median and STL filters reduced the uncertainty of SWE estimates, with average event uncertainty of ±1.1 cm and ±1.2 cm, respectively, and average dP_D errors of ±0.02 cm for both methods. This reduction in uncertainty improves the reliability of lake pressure SWE estimates, which we can validate with our manual observations.

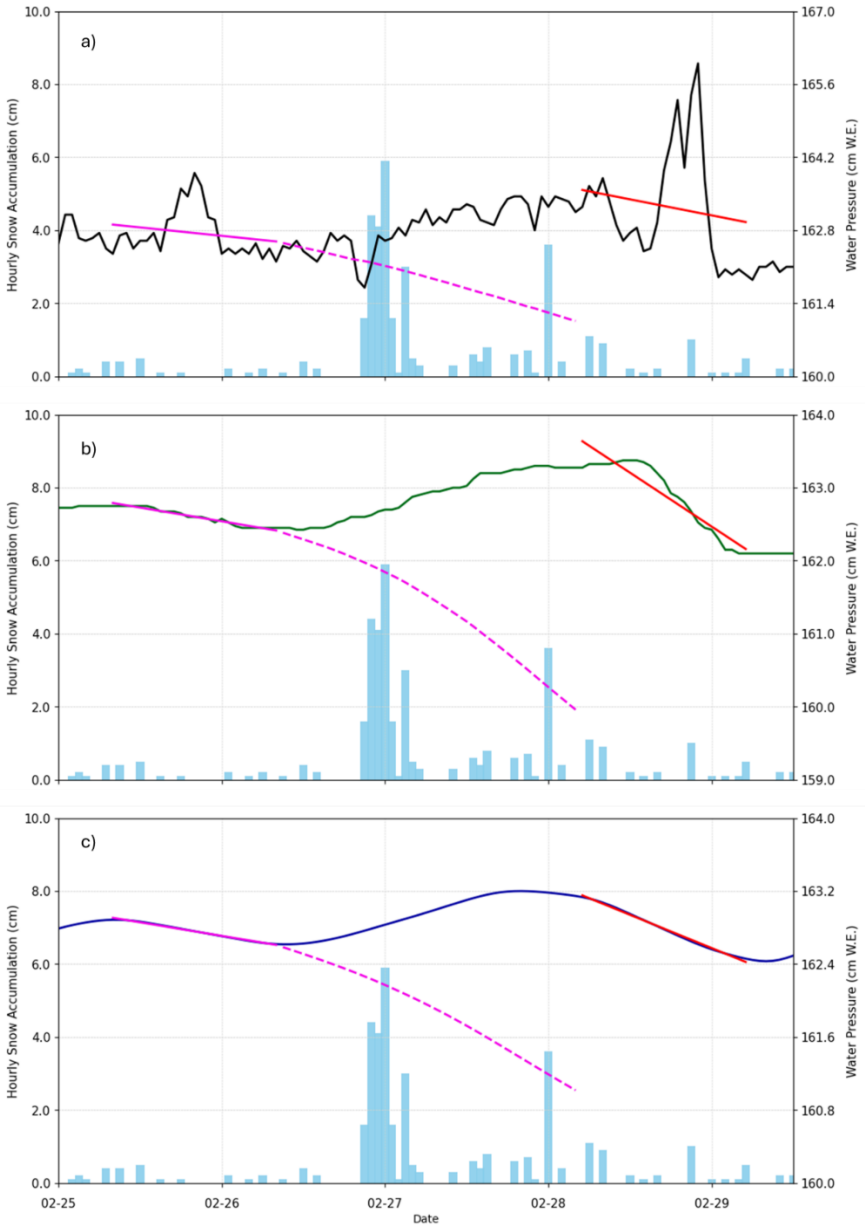


Figure 8. Estimation of pre-snow drainage (pink), post-snow drainage (green), and the total drainage component (dPD, dotted pink line) for Mystic Lake Average pressure shown for the February 26 snow event for raw pressure (a), moving median (b), and STL (c). Linear fit estimates for drainage rates are significantly improved by filtering the data.



Figure 9. Raw pressure (black), moving median (green), and STL (blue) time series displaying a continued decreasing trend during snow events on March 24 and March 26-27. The pressure response to snow loading was likely muted due to a partially unfrozen lake surface.

3.3 Manual observations

Each visit to the field site required a roundtrip from the trailhead of 20km with backcountry skis or 36km with cross-country skis. Due to the extensive travel component, the total number of manual samples each day varied based on time, weather conditions, and team capacity (Table 2). The results of the manual observations reveal different patterns of accumulation on the lake surface and ground surfaces at the field site (Figure 10). SWE and depth show a steady increase throughout the study period over the ground surfaces, with the highest recorded values of 51.5cm depth and 12cm SWE on March 27. The highest recorded values over the lake surface, however, were on February 17 with 22.5cm depth and 4cm SWE. On March 20, after 5 consecutive days of daily maximum air temperatures exceeding 15° C, the lake surface was completely free of snow with areas of standing water present. Despite the different temporal patterns of

accumulation found over the lake and ground surfaces, we did observe some notable similarities. Two snow events occurred between March 20 and 27, in which an increase in 3cm SWE was observed over both the lake and ground surfaces (Figure 10 and 11) and an increase in snow depth of 8cm and 10.5cm, respectively. The temporal pattern of snow density, excluding March 20, was more comparable between the lake and ground surfaces with a mean difference of 0.04 (4% water content).

February 01		February 17		February 28		March 20		March 27	
Ground	Lake	Ground	Lake	Ground	Lake	Ground	Lake	Ground	Lake
25	10	10	16	18	20	27	0	28	10

Table 2. Count of manual SWE and depth observations collected during each sampling date. Sample size varies based on team capacity for each day, and no samples were collected on March 20 over the lake surface due to standing water and hazardous ice conditions.

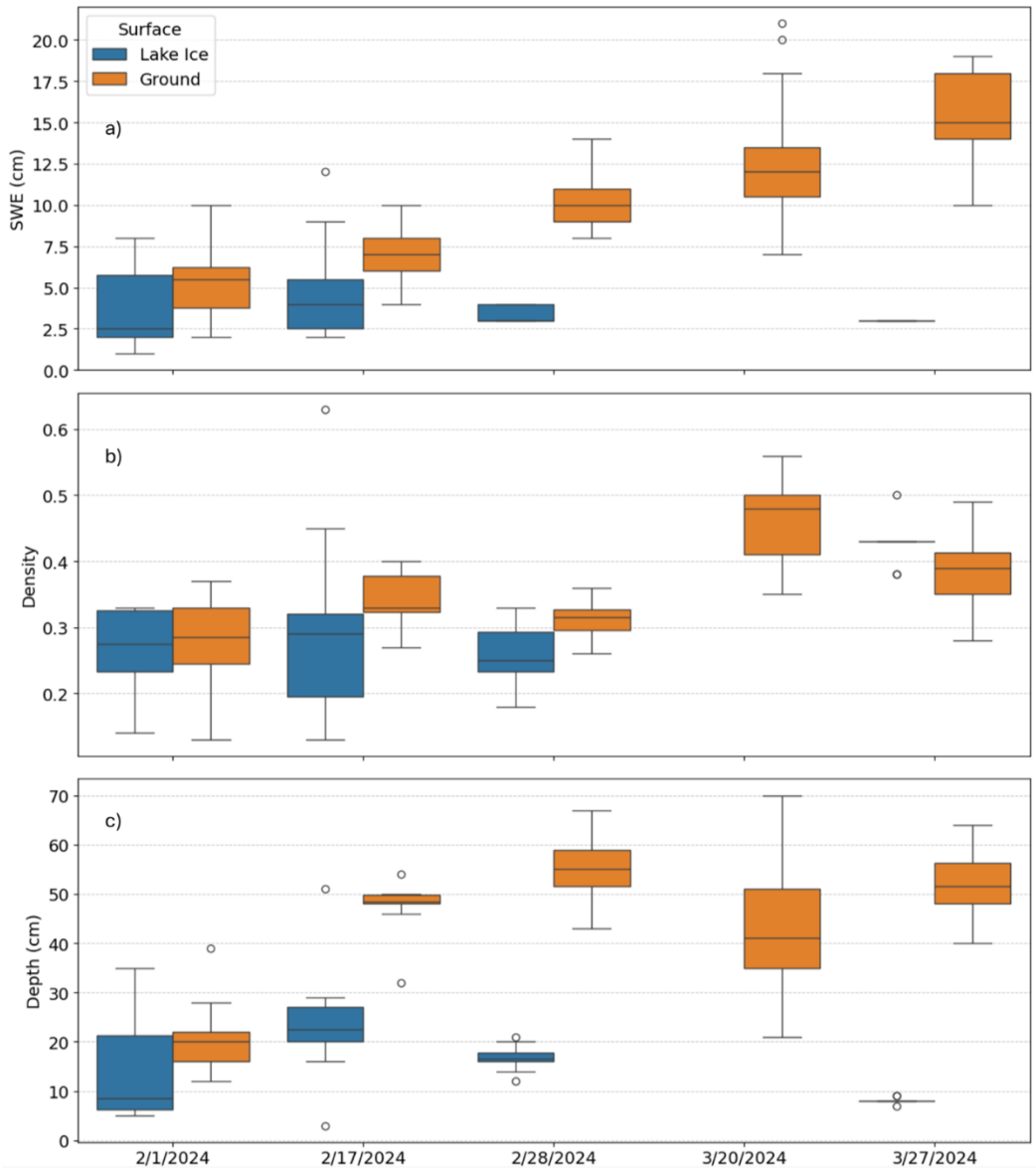


Figure 10. Box plots of SWE (a), density (b), and depth (c) recorded by sampling date and surface. Density was back calculated from SWE and depth. Ground surfaces steadily accumulated snow throughout the study, while the lake surface reaches a maximum SWE and depth on February 17.

Due to the constant, natural drainage from Mystic Lake, the lake pressure method can only produce SWE estimates when a clear pressure increase, distinct from the decreasing trend, can be attributed to snow accumulation. Furthermore, any natural loss of the snowpack from

sublimation, wind transport, and melt are not captured in the pressure signal. To account for this limitation and to assess the accuracy of SWE estimates using our manual samples, we calculate SWE from lake pressure for each site visit date by taking the cumulative SWE estimated from individual events and compare the observed changes in cumulative SWE in between site visits (Figure 11).

For individual periods in between site visits, represented by the different colored bars in Figure 11, the accuracy of lake pressure SWE estimates is variable. For the period between February 1 and 17, we found that all three pressure series overestimated SWE while the lake surface and ground surface samples yielded the same change of 1.5cm SWE. We believe that this overestimation results from the inability of the lake pressure method to capture natural snowpack loss, leading to a cumulative snow event SWE that is greater than the in-situ SWE. We again found agreement between the lake surface and ground surface samples for the period between March 20 and 27 with a change in 3cm SWE, but the lake pressure SWE estimates showed mixed results. Raw pressure greatly overestimated SWE for the March 20 to 27 period with an estimated change of 8.8cm SWE, which we believe resulted from significant noise in the data during this period (Figure 9). Moving median and STL, however, underestimated SWE observed by the manual samples. Since the lake surface was observed to be partially thawed on March 20, we interpret the underestimation to be the result of a dampened pressure response during the snow events. The variability in the accuracy of lake pressure SWE estimates between site visits highlights the limitations of this method in capturing natural snow loss and in capturing SWE during unsustained freezing conditions.

Compared to manual measurements over the lake surface, the raw, moving median, and STL pressure results overestimated SWE for the entire study period, which is represented by the total bar height in Figure 11. Manual samples over the lake surface show a decrease in SWE between February 17 and March 20, where all three lake pressure SWE estimates recorded increases during this period. Because the lake pressure method does not account for snowpack loss, the decreases in SWE observed on the lake surface between February 17 and March 20 were not captured in the pressure signal, resulting in an overestimation of SWE. Compared to the manual measurements over the ground surfaces, and SWE recorded at the Lick Creek SNOTEL site, we see that the filtered pressure yielded a much more accurate estimate for the entire study period. The cumulative SWE observed in the moving median and STL pressure series for the study period was 13.1 cm and 10cm, respectively, while the ground samples and Lick Creek SNOTEL yielded a SWE of 9.5cm and 10.4cm, respectively. The raw pressure data yielded 22.1cm SWE. The comparability of the filtered results to the ground samples and Lick Creek SNOTEL reveals two important findings. First, filtering the data produced a much more reliable estimate of SWE. Second, we were able to closely capture total SWE during the study period using the lake pressure method.

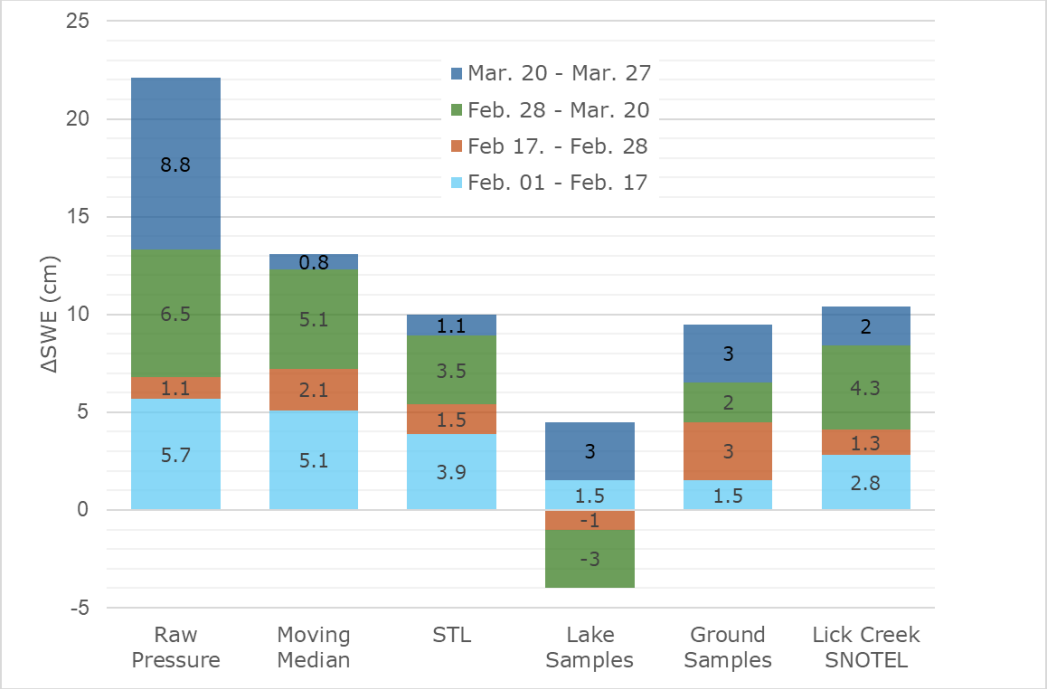


Figure 11. Change in SWE (ΔSWE) observed in between field sampling dates. The negative changes observed on the lake surface from Feb. 28 and Mar. 20 are the result of the complete loss of the lake surface snowpack. The height of each bar represents the total observed SWE on Mar. 27. All three water pressure series overestimate manual SWE observed on the lake surface, but STL pressure estimates most closely represent what was observed over the ground at the study site and at the Lick Creek SNOTEL site.

3.4 LiDAR snow depth

To evaluate how representative the lake pressure estimates are of the broader study area, we collected LiDAR snow depth measurements to assess spatiotemporal variability of the snowpack at a fine scale (50cm cell size). Snow depth was measured via LiDAR to assess the spatiotemporal variability of snow accumulation at 20cm resolution across the entire study site. Because of the difficulty and additional crew members required to haul in the equipment, LiDAR data was only obtained on February 1, March 20, and March 27. The LiDAR results show that the lake surface is representative of snow accumulation at the entire study site on February 1 and closely captured snow depth change from March 20 to 27 (Figure 12). The median snow depth

on the lake surface closely follows the median snow depth observed at the entire study site on February 1, at 9cm and 10cm, respectively. We found a median change in snow depth from March 20 to March 27 of 9cm at the entire study site and 8cm over the lake. Our manual samples support these findings, with the same observed change in SWE of 3cm observed over both the lake surface and ground surfaces (Figure 11).

The Mystic Lake study site is variable in slope aspect and vegetation cover, both of which have been shown to greatly impact snow accumulation (Tennent et al., 2017). Therefore, to better understand the spatial distribution and variability of snow accumulation at the site, we split the LiDAR results into slope aspect. We found that northern aspects, which are heavily forested at the site, accumulated more snow than eastern, southern, and western aspects at all site visits. This result is in agreement with previous research that demonstrates northern aspects in forested terrain can exhibit greater snow depths (Tennent et al., 2017). The maximum snow depth observed on March 27, is comparable between northern aspects and the flat meadow adjacent to Mystic Lake at 36cm and 35cm, respectively. The meadow is comprised of tall grasses and shrubs (~40cm in height), which have been shown to retain wind-drifting snow, potentially leading to an increased measured height of snow compared to neighboring forested areas (Sturm et al., 2001; Lamare et al., 2023). The AWS recorded the deepest snowpack throughout the entire study period with a maximum snow depth of 55cm (Figure 12). We believe that this is due to the location of the AWS in forest clearing. The dense canopy on northern aspects at the site may have intercepted incoming snow resulting in decreased accumulation at the ground (Varhola et al., 2010). Our finding suggests that forest clearings may have experienced less interception while still receiving protection from incoming solar radiation from the surrounding forest

(Varhola et al., 2010; Çitgez et al., 2024). Measuring the effects of forest density on snow accumulation is outside the scope of our study, but the LiDAR data supports this finding as forest clearings display greater snow depths than the adjacent forest (Figure 13). By splitting the LiDAR results into slope aspect, we highlight the challenges of measuring SWE in complex terrain. Although we found the lake surface to be representative of snow depth across the entire study site on February 1 and observed a similar change in snow depth from March 20 to 27, the lake surface displays an enhanced rate of snow loss that was not observed anywhere else at the study site.

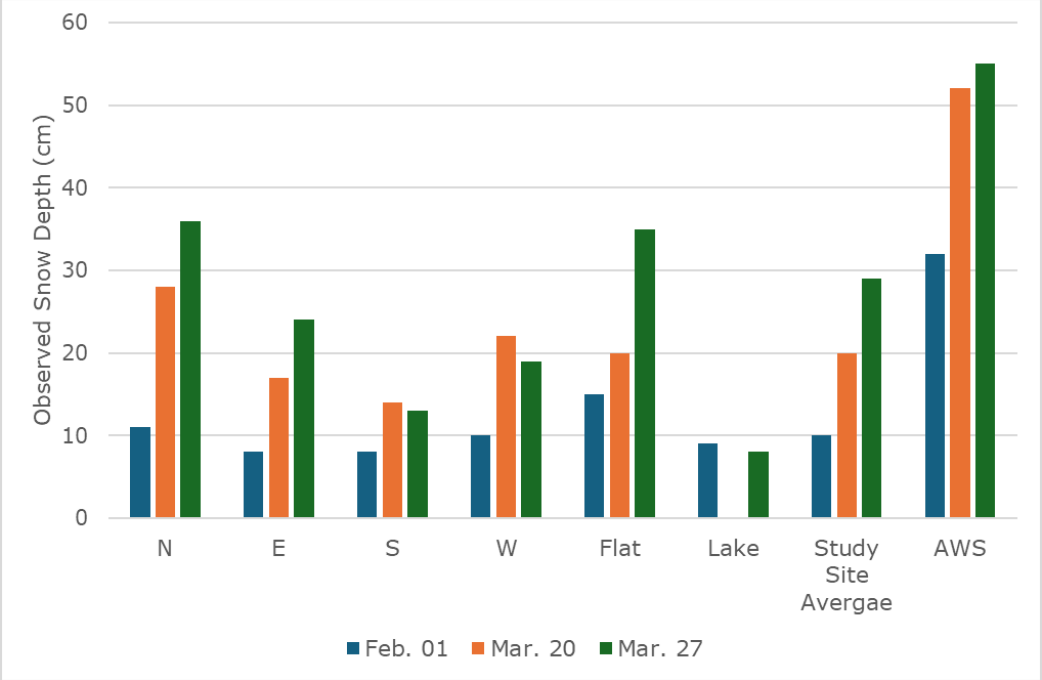


Figure 12. LiDAR snow depth, and snow depth recorded at the AWS, by sampling date. The location of the AWS in a forest clearing likely contributed to the deeper snowpack observed there relative to the rest of the study site. Snow depth over the lake surface was comparable to the study site on February 01 and experienced a similar increase in depth from March 20 to 27 of 8cm, compared to 9cm across the study site, but the loss of the snowpack over the lake surface on March 20 reveals an enhanced rate of snow loss not observed at any other area of the study site.

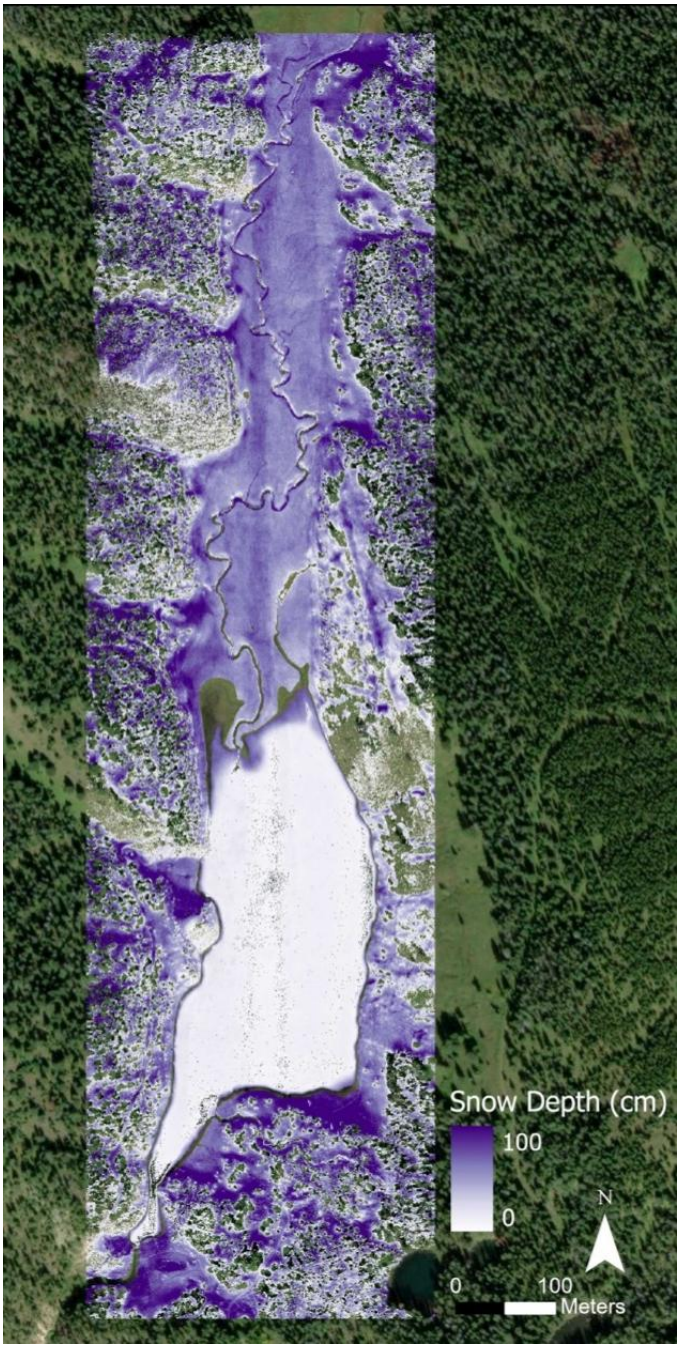


Figure 13. Snow depth retrieved from LiDAR on March 27. Vegetation and negative values are masked to highlight where snow is and is not present at the study site. The lake surface displays more homogenous snow depth compared to its surroundings. Forest clearings show the deepest snowpack in dark purple.

3.5 Loss of lake ice snowpack

The LiDAR and manual sample results show that, from February 17 to March 20, the lake surface snowpack disappeared. Although air temperatures were exceedingly warm prior to March 20, observations made during field sampling on February 17 and 28 implicate other possible mechanisms for the enhanced loss of the snowpack on the lake. On February 17 and 28, liquid water was present at the bottom of the lake surface snowpack with a layer of fully saturated snow above it, with an estimated thickness of ~5cm and ~15cm, respectively. We believe that the enhanced rate of snow loss observed over the lake ice, compared to ground surfaces, is the result of the introduction of liquid into the snowpack. It has been found that water upwelling through the ice, or depression of the ice below the lake water level, can increase snowmelt (Pouw et al., 2023). Warm temperatures also play a role in this mechanism by inhibiting the development of a thick layer of ice that would be more resistant to fracturing and depression (Liston and Hall, 1995; Wei et al., 2016; Sharma et al., 2024). Furthermore, it has been shown that open areas are subject to greater rates of sublimation due to increased solar radiation and wind exposure compared to adjacent forested areas (Svoma, 2015). It is likely that a combination of liquid water introduced from the lake below and sublimation from above resulted in the enhanced rate of snow melt on the lake surface.

4 Discussion

4.1 Future considerations

A pervasive theme that emerged was the warm winter temperatures and record low snow observed during the study period. As noted earlier, the 2024 winter season set the record low SWE at Lick Creek SNOTEL until March 2, where it barely hovered above the record low until a series of late spring snow events brought up peak SWE to 24.6cm, which is still well below the median peak SWE at Lick Creek SNOTEL of 30.7cm. The median winter temperature at the Lick Creek SNOTEL site for the period of record (1982) is -2.3°C, and the 2024 median temperature was -1.2°C. Additionally, ~34% of total hourly temperature readings recorded at the AWS, between November 2023 and March 2024, were above 0°C. The combination of warm temperatures and low snow presented several challenges in our study, but the largest challenge brought on by the tough conditions may have been the diurnal pressure cycle. Addressing noisy water pressure data was not an expected outcome in this study, yet we found it to be a necessary step to produce reliable SWE estimates. Through the application of moving median and STL filters we were able to produce more reliable and accurate SWE estimates from lake water pressure during difficult study period conditions. The relative success of filtering the data in this study presents a framework for handling noise in future studies and applications of the lake pressure SWE method.

Although noise from the diurnal cycle is highly correlated to temperature, an unknown source of uncertainty in the pressure signal is surface inflow and groundwater exchange. It was observed that multiple inlets into Mystic Lake flowed continuously throughout the winter, and that the lakebed was comprised of a deep layer of sediment which may have had multiple effects on

groundwater flow dynamics (Genereux and Bandopadhyay, 2001). The granitic surface geology of the Sierra Nevada Mountains in California and Beartooth Mountains in Montana, for example, may serve as ideal locations to implement the lake pressure SWE method in lakes with minimal groundwater and surface inflow at higher elevations (Armengol et al., 2024). Selecting such sites may help mitigate any unknown noise introduced by groundwater exchange and surface water inflow.

The spatial representativeness of lake pressure SWE estimates may also be improved by careful site selection. The results of our study showed that snow accumulation varied significantly by aspect at Mystic Lake, and it has been shown that more homogenous terrain exhibits less variability in SWE than areas with more complex topography (Skaugen and Melvold, 2019). Both the Sierra Nevada and Beartooth Mountains offer homogeneous, high elevation plateau settings in which lake pressure SWE estimates may be representative of a larger area.

We found that snow density over the lake surface was more comparable than depth or SWE to that of the surrounding study area, which is supported by a body of work that shows snow depth and SWE vary more in space than snow density (Elder et al., 1991; Sturm et al., 2010; López-Moreno et al., 2013; Meehan et al., 2024). Using spatially distributed bulk density estimates has been widely shown to improve the accuracy of SWE models (Sturm et al., 2010; Venäläinen et al., 2021; Meehan et al., 2024). Obtaining bulk snow density, however, requires SWE and snow depth measurements, and the difficulty of measuring SWE means it is observed spatially far less than depth. We have shown in this study that the lake pressure method provides valuable and easy-to-implement SWE measurements that could fill this data gap. Used in conjunction with a variety of continuous snow depth measuring techniques, the lake pressure method could be

applied to produce bulk snow density estimates that could greatly improve the accuracy of spatially distributed SWE models. Some complimentary depth measurement techniques are the use of remote cameras that employ a virtual snow stake (Strickfaden et al., 2023) to minimize installations and reduce costs, a noted benefit of the lake pressure method. Using tower mounted LiDAR to capture snow depth is an emerging approach (Lundquist et al., 2024) that could be installed to continuously measure depth over both a portion of a lake surface and adjacent ground surface. Commercial airborne LiDAR operations can accurately measure submeter variations in snow depth across large basins (Painter et al., 2016). This method is temporally restricted, but the use of satellite products like stereo imagery (Hu et al., 2023) and ICESat-2 retrievals (Besso et al., 2024) offer more frequent depth observations at coarser spatial resolutions.

4.1 Limitations

A key limitation of SWE estimates derived from lake pressure is that it is subject to human error. We manually determined the time periods for the pre-snow and post-snow drainage rate, as well as the duration of the snow event. For a snow event that occurred on February 26, increasing the duration of the snow event by 3 hours increased the raw pressure SWE estimate from 1.1cm to 3.3cm. Applying this same change to the moving median and STL filtered pressure yielded an increase in estimated SWE of 1.2cm and 0.2cm, respectively. Because the filtered data was not as influenced by the adjustment in snow event duration, we believe that SWE estimates from a less noisy pressure signal would be more robust to subjectivity. Although our study period presented us with a particularly noisy pressure signal, developing an approach to systematically identify snow event duration and pre-snow and post-snow drainage periods may reduce any error resulting from human subjectivity.

Sampling errors may have been introduced through our manual snow depth measurements. Although we initially planned a random sampling grid to minimize observational bias (Skøien and Blöschl, 2006), safety concerns in forested areas—where downed trees lay beneath shallow snowpacks—forced us to collect samples primarily in small forest clearings. As a result, our manual samples were biased toward locations with deeper snow, similar to the bias observed in AWS measurements. This is evident when comparing manual sample depths to LiDAR snow depth distributions (Figures 10 and 12), where our samples align more closely with AWS depths than with the study site's median snow depth. This sampling bias highlights the inherent difficulties in capturing snowpack variability, especially during low-snow years.

5 Conclusion

In this study, we investigated the accuracy and representativeness of SWE estimates derived from lake water pressure. We showed how noisy data can introduce considerable uncertainty in SWE estimates, and we greatly reduced this uncertainty by applying moving median and STL filters. We were able to closely represent SWE at the study site with the filtered pressure signals, but we highlight the limitations of the lake pressure method for capturing natural snowpack loss and snow events in unsustained freezing conditions. Although we find that snow accumulation on the lake ice surface is occasionally representative of the study site, an enhanced rate of snowpack loss, especially in winters with freeze- thaw-freeze cycles on the lake ice limits its spatiotemporal representativeness.

Through the challenges of working within a limited temporal scope during a warm, record-setting low snow period, we were able to further develop a framework of data filtering and site selection to improve the accuracy and spatial representation of the lake pressure method,

contributing valuable context for its refinement and application in SWE monitoring networks. Our study was limited to one winter, precluding a definitive result for the implementation of the lake pressure method at Mystic Lake. However, it presents a strong path forward for deploying this low-cost approach and identifies its limitations, a key component for advancing science (Firestein, 2015).

CONCLUSION

In this study, we investigated the accuracy and representativeness of SWE estimates derived from lake water pressure. We showed how noisy data can introduce considerable uncertainty in SWE estimates, and we greatly reduced this uncertainty by applying moving median and STL filters. We were able to closely represent SWE at the study site with the filtered pressure signals, but we highlight the limitations of the lake pressure method for capturing natural snowpack loss and snow events in unsustained freezing conditions. Although we find that snow accumulation on the lake ice surface is occasionally representative of the study site, an enhanced rate of snowpack loss, especially in winters with freeze- thaw-freeze cycles on the lake ice limits its spatiotemporal representativeness.

Through the challenges of working within a limited temporal scope during a warm, record-setting low snow period, we were able to further develop a framework of data filtering and site selection to improve the accuracy and spatial representation of the lake pressure method, contributing valuable context for its refinement and application in SWE monitoring networks. Our study was limited to one winter, precluding a definitive result for the implementation of the lake pressure method at Mystic Lake. However, it presents a strong path forward for deploying this low-cost approach and identifies its limitations, a key component for advancing science (Firestein, 2015).

CUMULATIVE REFERENCES CITED

Almazroui, Mansour, and Zekâi Şen. "Trend Analyses Methodologies in Hydro-Meteorological Records." Earth Systems and Environment 4.4 (2020): 713-38. Print.

Armengol, Sandra, et al. "Isogeochemical Characterization of Mountain System Recharge Processes in the Sierra Nevada, California." Water Resources Research 60.7 (2024): e2023WR035719. Print.

Bales, Roger C., et al. "Mountain Hydrology of the Western United States." Water Resources Research 42.8 (2006). Print.

Barnett, T. P., J. C. Adam, and D. P. Lettenmaier. "Potential Impacts of a Warming Climate on Water Availability in Snow-Dominated Regions." Nature 438.7066 (2005): 303-9. Print.

Besso, Hannah, David Shean, and Jessica D. Lundquist. "Mountain Snow Depth Retrievals from Customized Processing of Icesat-2 Satellite Laser Altimetry." Remote Sensing of Environment 300 (2024): 113843. Print.

Box, George E. P.; Jenkins, Gwilym M.; Reinsel, Gregory C.; Ljung, Greta M. . Time Series Analysis: Forecasting and Control,5th Edition, by George E. P. Box, Gwilym M. Jenkins, Gregory C. Reinsel and Greta M. Ljung, 2015. Published by John Wiley and Sons Inc., Hoboken, New Jersey, Pp. 712. Isbn: 978-1-118-67502-1. Journal of Time Series Analysis. 5th Edition ed. Vol. 37. Hoboken, New Jersey: John Wiley and Sons Inc., 2016. Print.

Burt, T. P., and J. J. McDonnell. "Whither Field Hydrology? The Need for Discovery Science and Outrageous Hydrological Hypotheses." Water Resources Research 51.8 (2015): 5919-28. Print.

Cho, E., et al. "Precipitation Biases and Snow Physics Limitations Drive the Uncertainties in Macroscale Modeled Snow Water Equivalent." Hydrol. Earth Syst. Sci. 26.22 (2022): 5721-35. Print.

Çitgez, Tarık, Remzi Eker, and Abdurrahim Aydın. "Spatio-Temporal Analysis of Snow Depth and Snow Water Equivalent in a Mountainous Catchment: Insights from in-Situ Observations and Statistical Modelling." Hydrological Processes 38.8 (2024): e15260. Print.

Cleveland, Robert B, et al. "Stl: A Seasonal-Trend Decomposition." J. off. Stat 6.1 (1990): 3-73. Print.

Dixon, David, and Sarah Boon. "Comparison of the Snowhydro Snow Sampler with Existing Snow Tube Designs." Hydrological Processes 26.17 (2012): 2555-62. Print.

Dozier, Jeff. "Mountain Hydrology, Snow Color, and the Fourth Paradigm." Eos, Transactions American Geophysical Union 92.43 (2011): 373-74. Print.

Dozier, Jeff, Edward H. Bair, and Robert E. Davis. "Estimating the Spatial Distribution of Snow Water Equivalent in the World's Mountains." WIREs Water 3.3 (2016): 461-74. Print.

Elder, Kelly, Jeff Dozier, and Joel Michaelsen. "Snow Accumulation and Distribution in an Alpine Watershed." Water Resources Research 27.7 (1991): 1541-52. Print.

Firestein, Stuart. Failure: Why Science Is So Successful. Oxford University Press USA, 2015. Print.

Genereux, D., and I. Bandopadhyay. "Numerical Investigation of Lake Bed Seepage Patterns: Effects of Porous Medium and Lake Properties." Journal of Hydrology 241.3 (2001): 286-303. Print.

Hammond, John C., et al. "High Resolution Snowmodel Simulations Reveal Future Elevation-Dependent Snow Loss and Earlier, Flashier Surface Water Input for the Upper Colorado River Basin." Earth's Future 11.2 (2023). Print.

Herbert, J. N., M. S. Raleigh, and E. E. Small. "Reanalyzing the Spatial Representativeness of Snow Depth at Automated Monitoring Stations Using Airborne Lidar Data." The Cryosphere 18.8 (2024): 3495-512. Print.

Hu, J. Michelle, David Shean, and Shashank Bhushan. "Six Consecutive Seasons of High-Resolution Mountain Snow Depth Maps from Satellite Stereo Imagery." Geophysical Research Letters 50.24 (2023): e2023GL104871. Print.

Immerzeel, W. W., et al. "Importance and Vulnerability of the World’s Water Towers." Nature 577.7790 (2020): 364-69. Print.

Kidmose, Jacob, et al. "Focused Groundwater Discharge of Phosphorus to a Eutrophic Seepage Lake (Lake Væng, Denmark): Implications for Lake Ecological State and Restoration." Hydrogeology Journal 21.8 (2013): 1787-802. Print.

Lamare, Maxim, et al. "Investigating the Role of Shrub Height and Topography in Snow Accumulation on Low-Arctic Tundra Using Uav-Borne Lidar." Journal of Hydrometeorology 24.5 (2023): 853-71. Print.

Li, Dongyue, et al. "The Value of Accurate High-Resolution and Spatially Continuous Snow Information to Streamflow Forecasts." Journal of Hydrometeorology 20.4 (2019): 731-49. Print.

Li, Dongyue, et al. "How Much Runoff Originates as Snow in the Western United States, and How Will That Change in the Future?" Geophysical Research Letters 44.12 (2017): 6163-72. Print.

Liston, Glen E., and Dorothy K. Hall. "An Energy-Balance Model of Lake-Ice Evolution." Journal of Glaciology 41.138 (1995): 373-82. Print.

López-Moreno, J. I., et al. "Small Scale Spatial Variability of Snow Density and Depth over Complex Alpine Terrain: Implications for Estimating Snow Water Equivalent." Advances in Water Resources 55 (2013): 40-52. Print.

López-Moreno, J. Ignacio, et al. "Intercomparison of Measurements of Bulk Snow Density and Water Equivalent of Snow Cover with Snow Core Samplers: Instrumental Bias and Variability Induced by Observers." Hydrological Processes 34.14 (2020): 3120-33. Print.

Meehan, T. G., et al. "Spatially Distributed Snow Depth, Bulk Density, and Snow Water Equivalent from Ground-Based and Airborne Sensor Integration at Grand Mesa, Colorado, USA." The Cryosphere 18.7 (2024): 3253-76. Print.

Miller, Z. S., et al. "Assessing the Seasonal Evolution of Snow Depth Spatial Variability and Scaling in Complex Mountain Terrain." The Cryosphere 16.12 (2022): 4907-30. Print.

Notarnicola, C. "Overall Negative Trends for Snow Cover Extent and Duration in Global Mountain Regions over 1982–2020." Scientific Reports 12.1 (2022): 13731. Print.

Painter, Thomas H., et al. "The Airborne Snow Observatory: Fusion of Scanning Lidar, Imaging Spectrometer, and Physically-Based Modeling for Mapping Snow Water Equivalent and Snow Albedo." Remote Sensing of Environment 184 (2016): 139-52. Print.

Pouw, A. F., H. Kheyrollah Pour, and A. MacLean. "Mapping Snow Depth on Canadian Sub-Arctic Lakes Using Ground-Penetrating Radar." The Cryosphere 17.6 (2023): 2367-85. Print.

Pritchard, H. D., D. Farinotti, and S. Colwell. "Measuring Changes in Snowpack Swe Continuously on a Landscape Scale Using Lake Water Pressure." Journal of Hydrometeorology 22.4 (2021): 795-811. Print.

Raleigh, Mark S., and Eric E. Small. "Snowpack Density Modeling Is the Primary Source of Uncertainty When Mapping Basin-Wide Swe with Lidar." Geophysical Research Letters 44.8 (2017): 3700-09. Print.

Sharma, S., et al. "Lake Ice from Historical Records to Contemporary Science." Journal of Geophysical Research: Biogeosciences 129.4 (2024): e2023JG007670. Print.

Siirila-Woodburn, Erica R., et al. "A Low-to-No Snow Future and Its Impacts on Water Resources in the Western United States." Nature Reviews Earth & Environment 2.11 (2021): 800-19. Print.

Skaugen, T., and K. Melvold. "Modeling the Snow Depth Variability with a High-Resolution Lidar Data Set and Nonlinear Terrain Dependency." Water Resources Research 55.11 (2019): 9689-704. Print.

Skøien, Jon Olav, and Günter Blöschl. "Sampling Scale Effects in Random Fields and Implications for Environmental Monitoring." Environmental Monitoring and Assessment 114.1 (2006): 521-52. Print.

Strickfaden, Kaitlyn M., et al. "Virtual Snow Stakes: A New Method for Snow Depth Measurement at Remote Camera Stations." Wildlife Society Bulletin 47.3 (2023): e1481. Print.

Sturm, Matthew, et al. "Snow–Shrub Interactions in Arctic Tundra: A Hypothesis with Climatic Implications." Journal of Climate 14.3 (2001): 336-44. Print.

Sturm, Matthew, et al. "Estimating Snow Water Equivalent Using Snow Depth Data and Climate Classes." Journal of Hydrometeorology 11.6 (2010): 1380-94. Print.

Svoma, Bohumil M. "Difficulties in Determining Snowpack Sublimation in Complex Terrain at the Macroscale." Advances in Meteorology 2016.1 (2016): 9695757. Print.

Taheri, Mercedeh, and Abdolmajid Mohammadian. "An Overview of Snow Water Equivalent: Methods, Challenges, and Future Outlook." Sustainability. 14.18 (2022). Web.

Tennant, Christopher J., et al. "Regional Sensitivities of Seasonal Snowpack to Elevation, Aspect, and Vegetation Cover in Western North America." Water Resources Research 53.8 (2017): 6908-26. Print.

van der Kamp, Garth, Dwayne Keir, and Marlene S. Evans. "Long-Term Water Level Changes in Closed-Basin Lakes of the Canadian Prairies." Canadian Water Resources Journal / Revue canadienne des ressources hydriques 33.1 (2008): 23-38. Print.

Wei, Lixin, et al. "The Impact of Meteorological Conditions on Snow and Ice Thickness in an Arctic Lake." Tellus A: Dynamic Meteorology and Oceanography (2016). Print.